Korean J. Chem. Eng., 34(8), 2162-2168 (2017)
DOI: 10.1007/s11814-017-0124-z

pISSN: 0256-1115
eISSN: 1975-7220

Facile synthesis of tungsten carbide-carbon composites for oxygen reduction reaction

Yeonsun Sohn, Jae Young Jung, and Pil Kim†

School of Semiconductor and Chemical Engineering, Nanomaterials Processing Research Center,
Chonbuk National University, Jeonju 54896, Korea
(*Received 2 February 2017 • accepted 1 May 2017*)

Abstract−Tungsten carbide-carbon composite (XWC-C, where X=10 or 30 represents the tungsten content) supports were prepared by pyrolyzing tungsten-adsorbed poly(4-vinylpyridine)-functionalized carbon. The supports were used to prepare Pt catalysts (Pt/XWC-C) for oxygen reduction reactions (ORR) in alkaline solution. Prepared XWC-C revealed highly dispersed tungsten carbide species composed of WC and W_2C phases. The tungsten carbide species proved to have a positive effect on the dispersion of Pt particles. Compared to the Pt catalyst supported on carbon (Pt/C), Pt/XWC-C showed higher ORR performance. In addition, the catalytic performance of Pt/XWC-C was enhanced with increasing tungsten carbide content. The highest ORR activity was achieved for the Pt/30WC-C catalyst, which had a 2.9-fold enhanced performance (at 0.8 V vs. RHE) compared to that of Pt/C. It is believed that the unique interaction between Pt and the tungsten carbide species was responsible for the enhanced ORR performance of the Pt/XWC-C catalysts.

Keywords: Tungsten Carbide, Composite Support, Oxygen Reduction Reaction (ORR), Pt Catalyst, Alkaline Fuel Cell

INTRODUCTION

Since the first report by Boudart et al. that transition metal carbides have similar electronic properties to those of noble metals such as Pt and Ru [1,2], substantial attention has been given to these carbides in an attempt to replace noble metals as catalysts [3-7]. In particular, tungsten carbide as an electrocatalyst has been extensively studied due to its Pt-like characteristics in the chemisorption of hydrogen and oxygen [8,9]. For example, a tungsten carbide nanostructure prepared by mechanical ball milling of WO_3, Mg, and C powders has been applied as an electrocatalyst in hydrogen oxidation reactions [10]. The catalytic performance achieved was fairly high considering that the tungsten carbide is a non-noble metal catalyst and other types of non-noble metals are almost inactive in hydrogen oxidation reactions. In another example, nanocrystalline tungsten carbide thin films were fabricated on Ni substrates for application in hydrogen evolution reactions [11-15]. Compared to Ni substrates, the prepared tungsten carbide thin films showed higher catalytic activity as well as electrochemical stability. Tungsten carbides have also been investigated as catalyst supports for Pt-based electrocatalysts [16-21]. Due to the characteristic valence of tungsten carbide and its strong resistance toward CO poisoning, this material is a promising catalyst support for the electro-oxidation of light hydrocarbon [22-24]. Lee et al. employed tungsten carbide-carbon (WC-C) microspheres as a support for Pt catalyst nanoparticles in the electro-oxidation of methanol [25,26]. The unique interaction between Pt and tungsten carbide was believed to have resulted in the enhanced catalytic performance of the Pt catalyst than when the catalyst was supported on a conventional carbon support.

On the other hand, oxygen reduction reactions (ORRs) in alkaline conditions would be the focus of much attention for the several important electrochemical energy conversion devices such alkaline fuel cells and metal-air batteries. Because the ORR kinetics in alkaline conditions, compared to those in acidic conditions, are relatively facile, the amount of Pt-based materials used for electrocatalysis can be decreased [27,28], leading to the improvement in the cost competitiveness of system. In addition, the stability of electrode materials at the oxidative potentials can be greatly enhanced in alkaline conditions, which makes it possible to design more durable electrode materials.

Tungsten carbides have been reported to be very effective in oxygen reduction reactions (ORRs) in alkaline solutions [29-31]. Several ORR studies have shown that the electrodes constructed with W_2C-modified Pt/C catalysts delivered higher kinetic currents than those made with Pt/C [32-35]. W_2C-modified Pt/C greatly reduced the overpotential as a result of the synergic effect of W_2C and Pt/C. The positive effect of tungsten carbide as a catalyst support is not limited to the case of Pt-based catalysts, as one ORR study demonstrated a similar synergic improvement of Ag supported on W_2C, indicating a strong advantage of tungsten carbide as a catalyst support [36].

There have been many reports on the preparation method for tungsten carbide, including WC-C composites [37-46]. Classically, tungsten carbides have been prepared by reacting tungsten oxide or tungsten metal with carbon sources at high temperatures under reducing atmospheres [47,48]. The resultant carbides usually exhibit low specific surface areas. However, tungsten carbide with high specific surface areas is recommended for catalytic applications. Several methods, including intermittent microwave heating [49,50],

†To whom correspondence should be addressed.
E-mail: kimpil1@chonbuk.ac.kr

carbothermal hydrogen reduction [51-53], and mechanical ball-milling [54,55], have been proposed to overcome this surface area disadvantage of tungsten carbides produced using classical preparation methods.

In this work, we present a very effective alternative for the preparation of carbon-supported tungsten carbide with a high surface area. A commercial carbon was functionalized with poly(4-vinylpyridine) (P4VP) that contains adsorption sites for tungsten and, at the same time, can serve as a carbon source for the formation of tungsten carbide. Prepared WC-C composites were applied as supports for Pt catalysts in ORRs in alkaline solution.

EXPERIMENTAL

1. Preparation of XWC-C Supports and Pt/XWC-C Catalysts

To prepare XWC-C (where X stands for the wt% of tungsten on carbon), a commercial carbon (Vulcan XC 72R, Cabot) was functionalized with P4VP. Briefly, an acid-treated Vulcan carbon (0.3 g) was dispersed in toluene (150 ml) by sonication for 30 min. Diluted 4-vinylpyridine (3 ml in toluene; Aldrich) followed by azobisisobutyronitrile (30 mg in toluene) were added to the mixture of toluene and carbon. Polymerization of 4-vinylpyridine was carried out at 70 °C for 24 hrs under a nitrogen atmosphere. The resultant mixture was filtered, washed with acetone, and dried at 50 °C for 12 hrs to yield P4VP-functionalized carbon (P4VP-C).

A WC-C composite was prepared using the P4VP-C as a substrate for the adsorption of tungsten. The P4VP-C (150 mg) was dispersed in ethanol solution of tungsten (VI) chloride (41 mg for 10WC-C; Aldrich). After stirring for 2 h at 25 °C, the resulting black mixture was filtered and washed with ethanol. The dried powder residue was subjected to heat-treatment at 850 °C for 5 hrs in a quartz tube under nitrogen atmosphere to produce 10WC-C. WC-C composites with different content of tungsten carbide can be prepared by changing the concentration of the tungsten precursor.

A 20 wt% Pt/XWC-C was prepared by a conventional borohydride reduction method as follows. The WC-C (100 mg) support was dispersed in an aqueous solution of the Pt precursor, H_2PtCl_6. An aqueous solution of $NaBH_4$ (6.9×10^{-2} M) was then added to the support-Pt precursor mixture under vigorous stirring. After further stirring for 2 hrs, the resultant slurry was filtered and washed with copious amounts of DI-water. The resultant black solid was dried at 100 °C for 24 hrs to yield the 20 wt% Pt/XWC-C catalyst. For the purpose of comparison, a 20 wt% Pt-supported on Vulcan carbon (Pt/C) was prepared by the same method as the Pt/XWC-C catalyst.

2. Characterizations and Measurement of the ORR Performance of the Catalyst

The morphologies of the supports and the catalysts were confirmed using transmission electron microscopy (TEM, JEOL-2010 installed in the Center for University-Wide Research Facilities (CURF) at Chonbuk National University). Functional groups on P4VP-C were identified with infra-red (IR, JASCO, FT/IR-4100). The crystalline phases of the supports and the catalysts were identified by x-ray diffraction (XRD, Rigaku D/MAX 2500) measurements using Cu-Ka radiation source (λ=1.54056 Å) operated at 40 kV and 30 mA.

Electrochemical performance of the prepared samples was measured with a conventional three-electrode cell. A Pt gauze and Hg/HgO (in 1 M NaOH) were used as the counter and the reference electrode, respectively. The working electrode was constructed with a catalyst ink-coated GC disk (diameter: 5.61 mm). The catalyst ink was prepared by the method reported previously in the literature [56]. To investigate the redox properties of prepared samples, cyclic voltammetry (CV) was conducted in an N_2-saturated 0.1 M KOH solution. The potential range was from −0.9 to 0.3 V and the scan rate was 50 mV/s. The ORR performances of the prepared samples were evaluated by conducting linear sweep voltammetry (LSV) in the range of 0.3~−0.7 V with a scan rate of 10 mV/s and a rotating ring disk electrode (RRDE, PINE(AFE7R9GCPT)) in a O_2-saturated KOH (0.1 M) solution. The ring potential was fixed at 0.3 V. To convert potential of Hg/HgO to that of reversible hydrogen electrode, the Hg/HgO was calibrated in H_2-purged 0.1 M KOH solution with Pt meshes as working and counter electrodes. The loading of the catalyst on the working electrode was 6.5 μg Pt/cm^2.

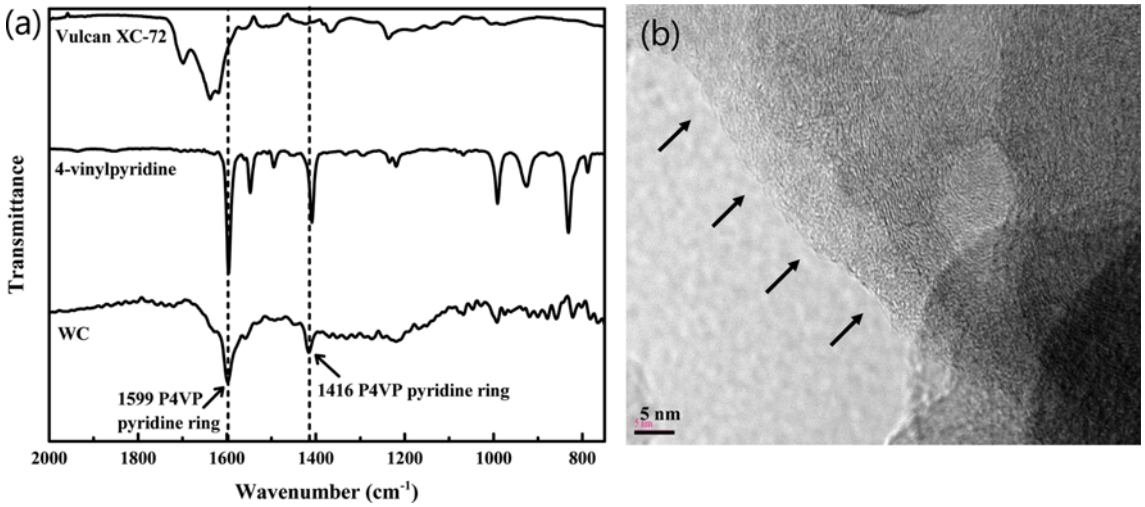

Fig. 1. (a) FT-IR spectra of bare carbon, pristine 4VP, and P4VP-functionalized carbon. (b) TEM image of P4VP-functionalized carbon.

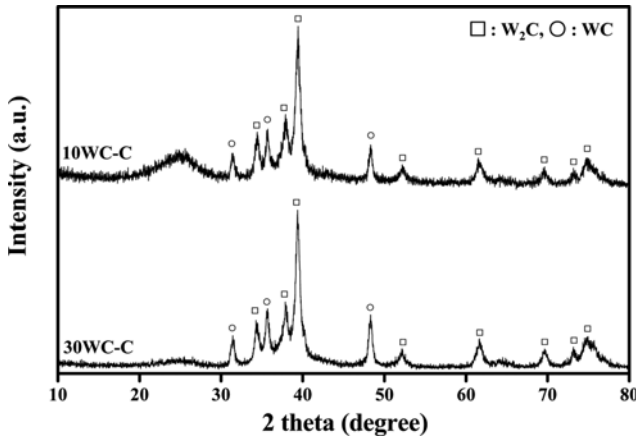

Fig. 2. XRD patterns of XWC-C.

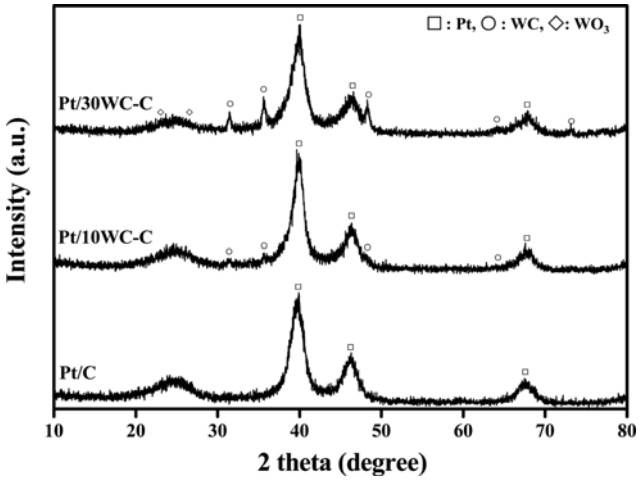

Fig. 4. XRD patterns of Pt/C and Pt/XWC-C catalysts.

RESULTS AND DISCUSSION

1. Properties of XWC-C and Pt/XWC-C

The functionalization of carbon with P4VP was confirmed by FT-IR spectroscopy and TEM analysis. The FT-IR spectra of bare carbon, pristine P4VP, and P4VP-C were compared in Fig. 1(a). Compared to bare carbon, P4VP-C was detected to have two characteristic peaks at 1,416 and 1,599 cm^{-1}, corresponding to the pyridine ring of P4VP, which is also identified in the spectrum of pristine P4VP. Furthermore, 4VP polymerized uniformly on the surface of carbon, as observed in Fig. 1(b). The carbon support employed was acid-treated before it was functionalized with P4VP. Acid treatment can produce various types of functional groups on the surface of carbon. The functional groups formed on the surface of carbon were characterized to have acidic proton that can interact with 4VP monomer. Therefore, the uniform functionalization of P4VP on the surface of carbon was derived from a strong interaction between 4VP monomer molecules and the functional groups on the surface of carbon.

Fig. 2 shows the XRD patterns of XWC-C. Characteristic peaks corresponding to the (021), (200), (121), (221), (040), (321), and (240) planes of W_2C crystal appeared at 34.3, 37.9, 39.4, 52.3, 62.1, 69.8, and 74.9° (2θ scale) [57]. Additional peaks at 31.3, 35.5, and 48.2° (2θ scale) were identified as the (001), (100), and (101) planes of the WC crystal [58]. No peak related to either tungsten trioxide or metallic tungsten was found in any sample. Therefore, it is believed that the main crystalline phases of WC-C supports consisted of only W_2C and WC.

Fig. 3 shows the W_2C and WC crystalline phases are uniformly dispersed on carbon. Tungsten carbides are conventionally prepared in high temperature conditions, where tungsten oxides are first reduced and subsequently reacted with a light hydrocarbon, such as methane, as a carbon source [59]. Resultant tungsten carbides were found to have relatively large sizes, probably because of sintering of the tungsten species during the high temperature treatment. Although the size of tungsten carbides in this study became slightly larger with increasing the tungsten content, a severe aggregation of tungsten carbides was not observed to occur as confirmed by the image of 30WC-C. This may have resulted from the interaction between the pyridinic groups of P4VP and the tungsten precursor molecules, mitigating the sintering of tungsten species during heat-treatment.

Fig. 4 shows the XRD patterns of the Pt/C and Pt/XWC-C catalysts. The diffraction peaks at 39.8, 46.2, and 67.4° respectively correspond to the (111), (200), and (222) planes of face-centered cubic crystalline Pt [60]. Any shift of the characteristic peak for Pt was not found in any sample, implying that a solid solution of Pt

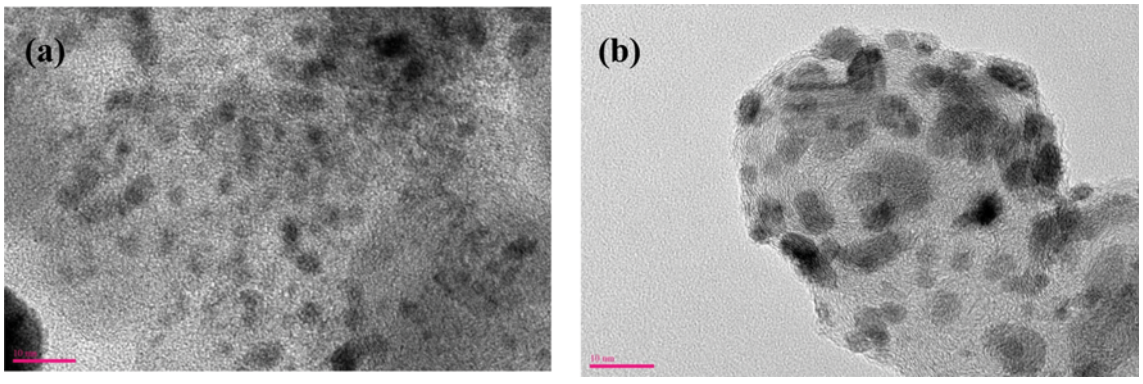

Fig. 3. TEM images of XWC-C.

Table 1. Particle size and surface area of Pt/C and Pt/XWC-C catalysts

Samples	Particle size (nm)	Surface area (m^2/g)
Pt/C	4.0	69.8
Pt/10WC-C	3.9	71.6
Pt/30WC-C	3.4	82.1

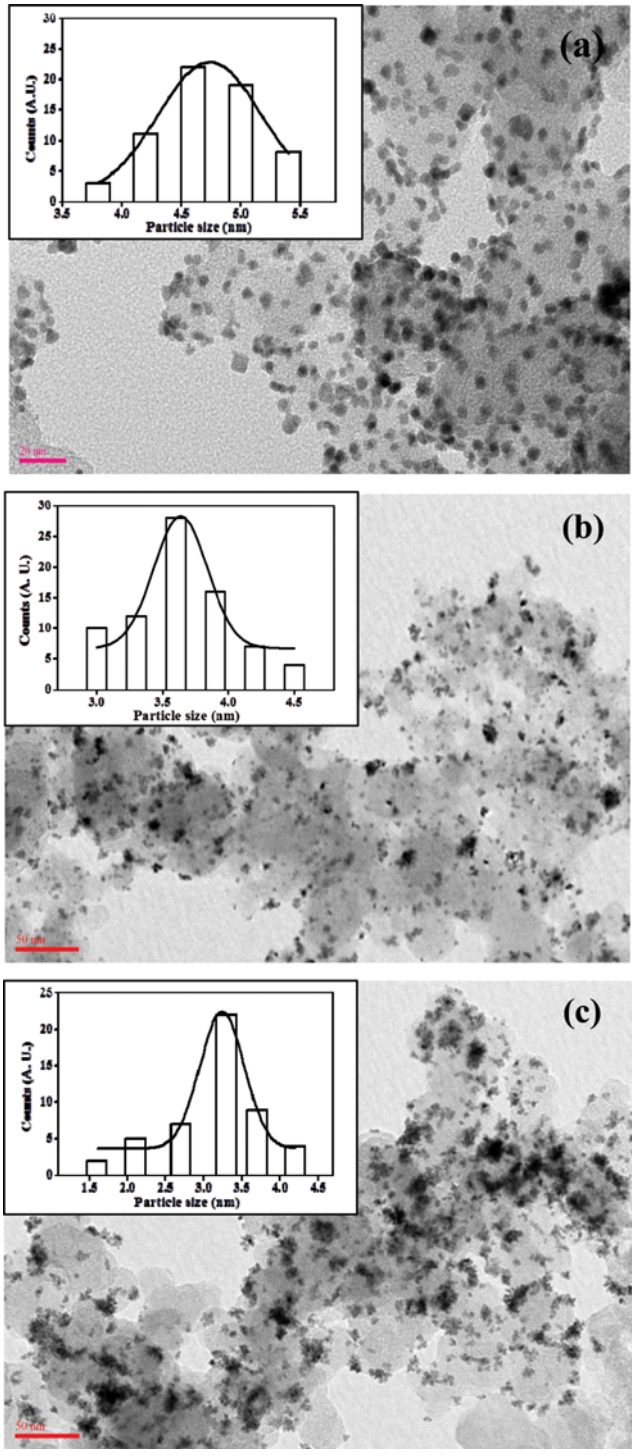

Fig. 5. TEM images of (a) Pt/C, (b) Pt/10WC-C, and (c) Pt/30WC-C. Insets represent the particle size distribution of Pt.

and W was not formed. The peaks at 31.5, 35.5, 48.2, and 64.2° for Pt/XWC-C correspond to the W_2C and WC crystalline phases, though their intensities were weak for Pt/10WC-C. This indicated that the tungsten carbide phases were retained after supporting Pt. By applying the Scherrer equation to the (220) diffraction peak, the particle size of Pt and the corresponding surface areas were calculated for each catalyst and are listed in Table 1. Compared to Pt/C, the Pt/XWC-C catalysts were calculated to have smaller Pt crystals and higher surface areas. Furthermore, the Pt size was slightly decreased with increasing content of tungsten carbides on carbon, indicating stronger interaction of Pt with the tungsten carbide species compared to that with carbon.

Fig. 5 shows TEM images and Pt particle size distributions (inset) of the Pt/C and Pt/XWC-C catalysts. Black dots, probably Pt, ranging from 3 to 4 nm in diameter, were observed in all samples, though they had different distributions depending on whether the tungsten carbides were also present on carbon. The trend for the Pt particle size was identical to that analyzed by XRD. The Pt/C catalyst had Pt nanoparticles that were uniformly dispersed on carbon. In contrast, the two Pt catalysts supported on XWC-C were observed to have small groups of Pt with dendrite-like structures. When considering the distribution of the tungsten carbide species on carbon, the unique dispersion and structure of Pt on Pt/XWC-C were likely due to the interaction between tungsten carbide and Pt. As shown in Fig. 5(b) and (c), it is clear that the interaction between Pt and tungsten carbide became extensive with increasing content of tungsten carbide. Note that this interaction has a positive influence on the size of Pt as confirmed by XRD analysis.

2. ORR Performance of Pt/C and Pt/XWC-C

To investigate the redox behavior of the prepared samples, CV was carried out in N_2-purged 0.1 M KOH solution. Fig. 6(a) shows CVs of the prepared samples including that of the 30WC-C support. Unlike Pt/C and Pt/XWC-C, the 30WC-C support does not show any particular peak and delivers negligible current in the range of −0.03~1.17 V. This indicates that the XWC-C support had a relatively high electrochemical stability in alkaline solution. The Pt/C and Pt/XWC-C catalysts exhibited typical characteristic currents [61]. In the anodic sweep, the current for the desorption of hydrogen appeared in the range of −0.03~0.4 V and the oxidation of Pt started at around 0.7 V, while in the cathodic sweep, the reduction peak of oxidized Pt species at around 0.7 V and the hydrogen adsorption current was observed in the range of 0.4~−0.03 V. The charge for the desorption of hydrogen, corresponding to the corrected integrated area contributed by double-layer charging current, is known to be closely related to the surface area of Pt [61]. Among the catalysts tested, Pt/30WC-C had the highest hydrogen desorption charge, while Pt/10WC-C was found to have a hydrogen desorption charge comparable to that of Pt/C. This is consistent with the tendency confirmed by XRD and TEM analyses, where the Pt particle size of the catalysts decreased from Pt/C≥Pt/10WC-C>Pt/30WC-C.

The catalytic performance of each prepared sample was evaluated by conducting LSV in O_2-saturated KOH solution. Fig. 6(b) shows the polarization curves that were obtained. Compared to Pt/C and Pt/XWC-C catalysts, the 30WC-C sample delivered lower current with higher overpotential for ORR, indicating an inferior ORR

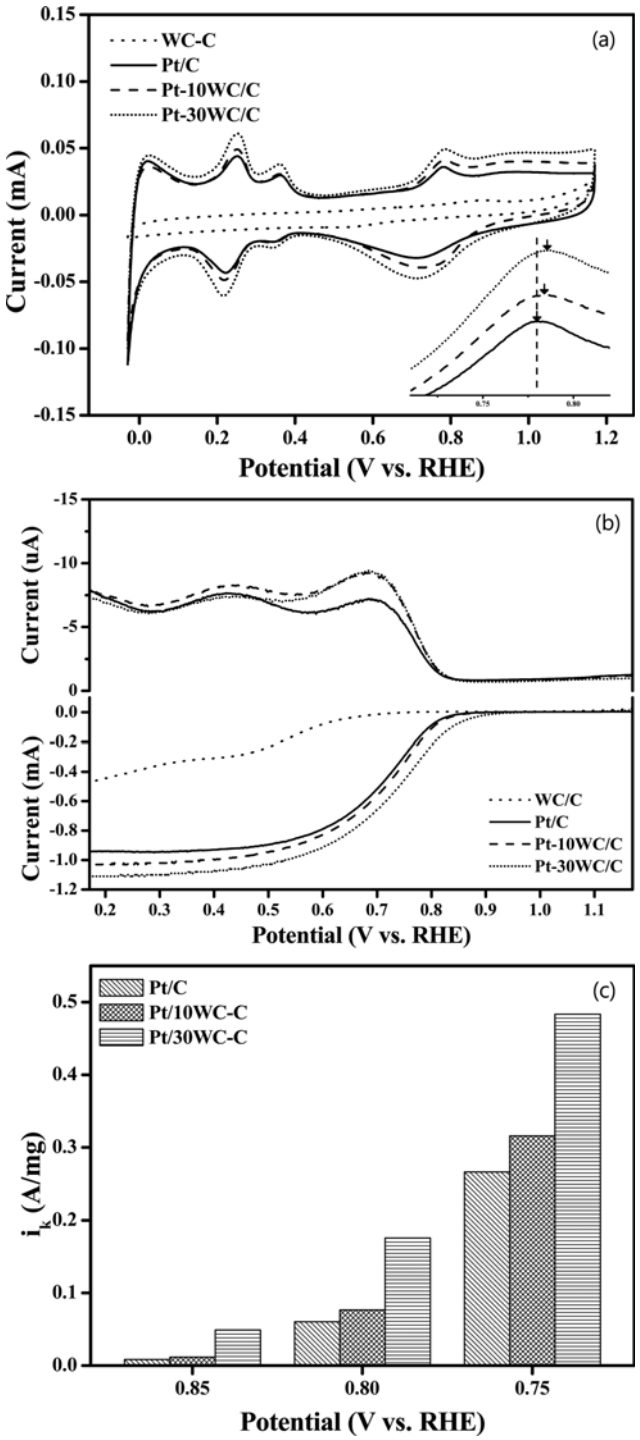

Fig. 6. (a) Cyclic voltammograms obtained with 30WC-C, Pt/C and Pt/XWC-C catalysts in N_2-saturated 0.1 M KOH solution. (b) Linear sweep voltammograms obtained with 30WC-C, Pt/C and Pt/XWC-C catalysts in O_2-saturated 0.1 M KOH solution. (c) Kinetic currents calculated at 0.85, 0.8, and 0.75 V (vs. RHE) over Pt/C and Pt/XWC-C catalysts.

performance of tungsten carbide alone. On the other hand, all Pt catalysts studied in this work exhibited similar patterns for both disk and ring currents. However, the catalysts had different half-wave potentials and onset potentials. The half-wave potential was measured to be 0.712, 0.715, and 0.729 V for Pt/C, Pt/10WC-C, and Pt/30WC-C, respectively. Furthermore, their onset potentials decreased from Pt/30WC-C>Pt/10WC-C>Pt/C. The observed half-wave potentials and onset potentials imply that the ORR performances had the following trend: Pt/30WC-C>Pt/10WC-C>Pt/C.

Quantitative evaluations of the catalytic performances were made based on the kinetic current. The kinetic current was calculated using the following equation: $i_k=i_L \bullet i/(i_L-i)$, where i_k, i_L, and i represent the kinetic current, limiting current, and measured current, respectively [62]. Fig. 6(c) presents the kinetic current calculated at 0.85, 0.80, and 0.75 V for Pt/C and Pt/XWC-C catalysts. The trend of kinetic current is similar to those of the half-wave potential and onset potential. Compared to Pt/C, the Pt/XWC-C catalysts were found to have higher kinetic current. In particular, the best ORR performance (at 0.8 V vs. RHE) was achieved using the Pt/30WC-C catalyst, which was 2.9- and 2.3-times better than those of Pt/C and Pt/10WC-C, respectively. The relatively higher ORR performance of the Pt/XWC-C catalysts compared to the Pt/C catalyst was partly due to the presence of the tungsten carbide species with intrinsic ORR activity as shown in Fig. 6(b), where the carbide species delivered an ORR current without Pt. However, the more crucial factor contributing to the enhancement in ORR performance of Pt/XWC-C probably resulted from the unique interaction between Pt and the tungsten carbide species, as confirmed by TEM analysis. It is well known that the ORR activity of Pt-based catalysts is enhanced as the oxidation of Pt is retarded, in which case more active sites on the Pt surface can be facilitated for ORR [63]. In our study, the interaction between Pt and tungsten carbide likely altered the oxidation resistance of Pt as confirmed in the inset of Fig. 6(a), in which the peaks of Pt oxidation are marked by arrows. The peak potential for the oxidation of Pt shifted to a higher potential as the WC content in the catalyst increased. This implies that the WC species made Pt more resistant toward oxidation and consequently more active in ORR. Besides this, the surface area of Pt likely contributed to the ORR activity of Pt as in the case of Pt/30WC-C, which revealed the highest surface area of Pt as evidenced in the XRD, TEM, and CV analyses.

CONCLUSIONS

Highly dispersed XWC-C (where X=10 or 30) were prepared as a support for Pt catalysts during ORR. P4VP introduced on the surface of carbon was facilitated not only for the adsorption of tungsten but also for the carbon source for the formation of tungsten carbide. The crystal structure of the prepared XWC-C supports was measured to have the mixed phases of WC and W_2C, and these phases were maintained after impregnation of Pt. It was revealed that the tungsten carbide species had a positive effect on the dispersion of Pt nanoparticles as the size of the Pt particles decreased with increasing tungsten carbide content, which resulted from the strong interaction between Pt and the tungsten carbide species. Also, the interaction between Pt and tungsten carbide played a crucial role in the enhanced performance of the Pt/XWC-C catalysts. The interaction between Pt and the tungsten carbide species became extensive as the content of tungsten carbide increased.

Consequently, the highest ORR activity (at 0.8 V vs. RHE) was achieved on Pt/30WC-C, which had a 2.9-fold enhanced performance compared to that of Pt/C.

ACKNOWLEDGEMENTS

This work was suppoted by the National Research Foundation of Korea (NRF) grant funded by the Korea government (MSIP) (No. 2015R1A2A2A01007622). This work was also supported by the New & Renewable Energy Core Technology Program of the Korea Institute of Energy Technology Evaluation and Planning (KETEP) grant funded by MOTIE, Republic of Korea (No. 20133030011320).

REFERENCES

1. R. L. Levy and M. Boudart, *Science*, **181**, 547 (1973).
2. F. H. Ribeiro, R. A. Dalla Betta, G. J. Guskey and M. Budart, *Chem. Mater.*, **3**, 805 (1991).
3. J. G. Chen, *Chem. Rev.*, **96**, 1477 (1996).
4. M. L. H. Green, T. Xiao, A. P. E. York and V. C. Williams, *Chem. Mater.*, **12**, 3869 (2000).
5. R. Venkataraman, H. R. Kunz and J. M. Fenton, *J. Electrochem. Soc.*, **150**, A287 (2003).
6. T. H. Nguyen, A. A. Adesina, E. M. T. Yue, Y. J. Lee, A. Khodakov and M. P. Brungs, *J. Chem. Technol. Biot.*, **79**, 286 (2004).
7. J. D. Oxley, M. M. Mdleleni and K. S. Suslick, *Catal. Today*, **88**, 139 (2004).
8. X. G. Yang and C. Y. Wang, *Appl. Phys. Lett.*, **86**, 224104 (2005).
9. A. R. Ko, Y. W. Lee, J. S. Moon, S. B. Han, G. Cao and K. W. Park, *Appl. Catal. A-Gen.*, **477**, 102 (2014).
10. H. H. Nersisyan, H. I. Won and C. W. Won, *Mater. Lett.*, **59**, 3950 (2005).
11. H. Zheng, J. Huang, W. Wang and C. Ma, *Electrochem. Commun.*, **7**, 1045 (2005).
12. M. Shaobo, Y. Yezhi, W. longbiao, W. Jun and H. Qinggan, *J. Chem. Phys.*, **13**, 487 (2000).
13. C. Tianyi, Z. Bohong, C. Wenbo and L. Yao, *Electrochemistry*, **3**, 343 (2002).
14. N. Ji, T. Zhang, M. Zheng, A. Wang, H. Wang, X. Wang and J. G. Chen, *Angew. Chem. Int. Edit.*, **120**, 8638 (2008).
15. N. C. Adriana, A. S. M. Sergio and A. A. Luis, *Electrochem. Commun.*, **1**, 600 (1999).
16. Y. Wang, S. Song, V. Maragou and P. K. Shen, *Appl. Catal. B: Environ.*, **89**, 223 (2009).
17. H. Chhina, S. Campbell and O. Kesler, *J. Power Sources*, **179**, 50 (2008).
18. J. B. Joo, J. S. Kim, P. Kim and J. Yi, *Mater. Lett.*, **62**, 3497 (2008).
19. C. Ma, J. Sheng, N. Brandon, C. Zhang and G. Li, *Int. J. Hydrogen Energy*, **32**, 2824 (2007).
20. Y. Liu and W. E. Mustain, *ACS Catal.*, **1**, 212 (2011).
21. H. Chhina, S. Campbell and O. Kesler, *J. Power Sources*, **164**, 431 (2007).
22. G. Cui, P. K. Shen, H. Meng, J. Zhao and G. Wu, *J. Power Sources*, **196**, 6125 (2011).
23. Z. J. Mellinger, E. C. Weigert, A. L. Stottlemyer and J. G. Chen, *Electrochem. Solid State Lett.*, **11**, B63 (2008).
24. T. E. Shubina and M. T. M. Koper, *Electrochim. Acta*, **47**, 3621 (2002).
25. R. Ganesan and J. S. Lee, *Angew. Chem. Int. Edit.*, **44**, 6557 (2005).
26. R. Ganesan and J. S. Lee, *J. Power Sources*, **157**, 217 (2006).
27. S. Zhao, A. E. Wangstrom, Y. Liu, W. A. Rigdon and W. E. Mustain, *Electrochim. Acta*, **157**, 175 (2015).
28. B. B. Blizanac, P. N. Ross and N. M. Markovic, *Electrochim. Acta*, **52**, 2264 (2007).
29. H. Meng and P. K. Shen, *Electrochem. Commun.*, **8**, 588 (2006).
30. N. R. Elezovic, B. M. Babic, L. Gajic-Krstajic, P. Ercius, V. R. Radmilovic, N. V. Krstajic and L. M. Vracar, *Electrochim. Acta*, **69**, 239 (2012).
31. H. Meng and P. K. Shen, *Chem. Commun.*, **1**, 4408 (2005).
32. J. R. Varcoe and R. C. T. Slade, *Fuel Cells*, **5**, 187 (2005).
33. X. Ma, H. Meng, M. Cai and P. K. Shen, *J. Am. Chem. Soc.*, **134**, 1954 (2012).
34. H. Meng and P. K. Shen, *J. Phys. Chem. B*, **109**, 22705 (2005).
35. P. N. Ross and P. Stonehart, *J. Catal.*, **48**, 42 (1977).
36. H. Meng, M. Wu, X. X. Hu, M. Nie, Z. D. Wei and P. K. Shen, *Fuel Cells*, **6**, 447 (2006).
37. W. Zhu, A. Ignaszak, C. Song, R. Baker, R. Hui, J. Zhang, F. Nan, G. Botton, S. Ye and S. Campbell, *Electrochim. Acta*, **61**, 198 (2012).
38. E. C. Weigert, A. L. Stottlemyer, M. B. Zellner and J. G. Chen, *J. Phys. Chem. C*, **111**, 14617 (2007).
39. E. C. Weigert, D. V. Esposito and J. G. Chen, *J. Power Sources*, **193**, 501 (2009).
40. H. H. Hwu, K. Kourtakis, J. G. Lavin and J. G. Chen, *J. Phys. Chem. B*, **105**, 10037 (2001).
41. M. B. Zellnera and J. G. Chen, *J. Electrochem. Soc.*, **152**, A1483 (2005).
42. N. Liu, K. Kourtakis, J. C. Figueroa and J. G. Chen, *J. Catal.*, **215**, 254 (2003).
43. D. J. Ham, Y. K. Kim, S. H. Han and J. S. Lee, *Catal. Today*, **132**, 117 (2008).
44. H. Zheng, Z. Gu, J. Zhong and W. Wang, *J. Mater. Sci. Technol.*, **23**, 591 (2007).
45. M. K. Jeona, K. R. Lee, W. S. Lee, H. Daimon, A. Nakahara and S. I. Woo, *J. Power Sources*, **185**, 927 (2008).
46. C. A. Angelucci, L. J. Deiner and F. C. Nart, *J. Solid State Electrochem.*, **12**, 1599 (2008).
47. N. Keller, B. Pietruszka and V. Keller, *Mater. Lett.*, **60**, 1774 (2006).
48. H. E. Sliney, *Tribol. Int.*, **15**, 303 (1982).
49. F. P. Hu, F. W. Ding, S. Q. Song and P. K. Shen, *J. Power Sources*, **163**, 415 (2006).
50. M. Nie, P. K. Shen and Z. D. Wei, *J. Power Sources*, **167**, 69 (2007).
51. M. J. Hudson, J. W. Peckett and P. J. F. Harris, *Ind. Eng. Chem. Res.*, **44**, 5575 (2005).
52. C. Liang, F. Tian, Z. Wei, Q. Xin and C. Li, *Nanotechnology*, **14**, 9 (2003).
53. R. Koc and S. K. Kodambaka, *J. Eur. Ceram. Soc.*, **20**, 1859 (2000).
54. G. M. Wang, S. J. Campbell, A. Calka and W. A. Kaczmarek, *J. Mater. Sci.*, **32**, 1461 (1997).
55. F. L. Zhang, M. Zhu and C. Y. Wang, *Int. J. Refract. Met. H.*, **26**, 329 (2008).
56. S. Beak, D. Jung, K. S. Nahm and P. Kim, *Catal. Lett.*, **134**, 288 (2010).

57. C. B. Rodella, D. H. Barrett, S. F. Moya, S. J. A. Figueroa, M. T. B. Pimenta, A. A. S. Curvelo and V. T. Silva, *RSC Adv.*, **5**, 23874 (2015).
58. R. Wang, C. Tian, L. Wang, B. Wang, H. Zhang and H. Fu, *Chem. Commun.*, **1**, 3104 (2009).
59. D. G. Barton, S. L. Soled and E. Iglesia, *Top. Catal.*, **6**, 87 (1998).
60. D. Jung, S. Beak, K. S. Nahm and P. Kim, *Korean J. Chem. Eng.*, **27**, 1689 (2010).
61. B. Li and J. Prakash, *Electrochem. Commun.*, **11**, 1162 (2009).
62. S. J. Bae, S. J. Yoo, Y. Lim, S. Kim, Y. Lim, J. Choi, K. S. Nahm, S. J. Hwang, T. H. Lim, S. K. Kim and P. Kim, *J. Mater. Chem.*, **22**, 8820 (2012).
63. Y. Hara, N. Minami, H. Matsumoto and H. Itagaki, *Appl. Catal. A-Gen.*, **332**, 289 (2007).